Temperature-insensitive photonic crystal fiber interferometer for absolute strain sensing

Joel Villatoro[a] and Vittoria Finazzi
ICFO-Institut de Ciències Fotóniques, Parc Mediterrani de la Tecnologia, Av. del Canal Olímpic s/n, Castelldefels, 08860 Barcelona, Spain

Vladimir P. Minkovich
Centro de Investigaciones en Óptica A. C., Loma del Bosque 115 León, 37150 Guanajuato, Mexico

Valerio Pruneri[b] and Gonçal Badenes
ICFO-Institut de Ciències Fotóniques, Parc Mediterrani de la Tecnologia, Av. del Canal Olímpic s/n, Castelldefels, 08860 Barcelona, Spain

(Received 15 June 2007; accepted 2 August 2007; published online 27 August 2007)

The authors report a highly sensitive (~2.8 pm/$\mu\varepsilon$) wavelength-encoded strain sensor made from a piece of photonic crystal fiber (PCF) spliced to standard fibers. The authors intentionally collapse the PCF air holes over a short region to enlarge the propagating mode of the lead-in fiber which allows the coupling of only two modes in the PCF. The transmission spectrum of the interferometer is stable and sinusoidal over a broad wavelength range. The sensor exhibits linear response to strain over a large measurement range, its temperature sensitivity is very low, and for its interrogation a battery-operated light emitting diode and a miniature spectrometer are sufficient. © *2007 American Institute of Physics*. [DOI: 10.1063/1.2775326]

There are a number of applications of practical interest in which the monitoring of strain-induced changes is important. Two typical examples include the status or health monitoring of complex structures such as aerospace, marine, or civil structures, and the curing process of composite materials. All these applications had led to today's fastest developing optical fiber strain sensors. To date a number of designs based on standard optical fiber have been reported in the literature; however, strain sensors based on in-fiber gratings[1] and Brillouin scattering[2] have proved to be useful and are commercially available. An enduring drawback of these strain sensors is their undesirable thermal sensitivity. To address this issue one has to design sensing heads with athermal packages or to simultaneously and independently measure strain and temperature.[1,2] In either case the complexity of the sensor is increased.

The advent of photonic crystal fibers[3] (PCFs) has motivated the research on alternative approaches to sense strain; Brillouin frequency shift,[4] Bragg or long-period gratings,[5–8] and modal interferometers[9–14] are some examples. In most of these approaches[4–10] the temperature dependence is still an unwelcome effect that has yet to be addressed. An important drawback of strain sensors based on PCF interferometers[9–14] reported so far is their relative complexity (critical launching or polarization conditions, need of still unavailable passive PCF devices, or incompatibility with standard fibers) that severely limits their practical applications. Here we propose a simple and robust two-mode interferometer that consists of a piece of PCF fusion spliced to two conventional single mode fibers. The interferometer exploits the modal properties of PCFs with the advantage that its interrogation is carried out with common optical fibers. The device exhibits a truly sinusoidal interference pattern over a broad wavelength range (~800 nm) which shifts linearly with the applied strain. The interrogation of the device is fast (in the millisecond range) and simple since just a low-power light emitting diode (LED) and a medium-resolution spectrometer are needed.

Figure 1 shows the proposed interferometer for strain sensing. It consists of a short piece of index-guiding PCF (Refs. 11 and 12) longitudinally sandwiched between two standard single mode fibers (SMFs) of the same type. The external diameter of both the PCF and the SMF was 125 μm. The PCF has five rings of air holes with a missing hole at the center that plays the role of core.[11,12] The fabrication of the interferometer only involves cleaving and fusion splicing, processes that are carried out automatically with common fiber optics instruments. The default programs for splicing SMFs were used in order to fabricate robust devices. Under these conditions the air holes of the PCF are tapered, over a length of approximately 90 μm, and then, they get completely collapsed. The high-strength fusion splices are converted permanently into a solid piece of silica whose overall length is approximately 400 μm.

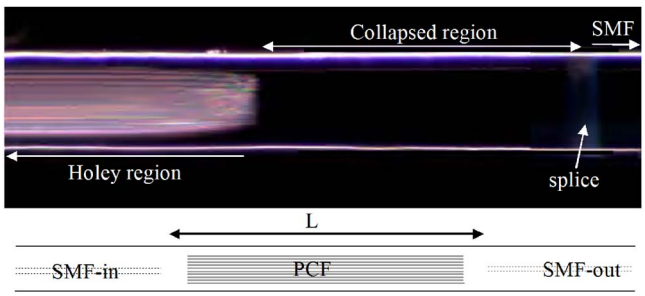

FIG. 1. (Color online) Photograph of a section of the splice. The image shows that the PCF voids are tapered in a short region before getting fully collapsed. The bottom drawing is a schematic diagram of the interferometer. SMF stands for single mode fiber, PCF for photonic crystal fiber, and *L* is the length of PCF.

[a]Electronic mail: joel.villatoro@icfo.es
[b]Also at: ICREA-Institució Catalana de Recerca i Estudis Avançats, 08010 Barcelona, Spain.

The propagating mode of the lead-in SMF diffracts, regardless the wavelength, as it enters the solid region (splice). Owing to diffraction the mode broadens but it never reaches the external PCF surface.[12] The enlarged mode then penetrates into a zone of tapered voids and finally reaches the PCF. The collapsed region and the tapered voids within the PCF are responsible for the excitation of two modes in the PCF.[12] Assuming that only two modes are excited the accumulated phase difference between them is $2\pi\Delta nL/\lambda$, where $\Delta n=n_1-n_2$, with n_1 and n_2 the effective indices of the two interfering modes, L is the length of PCF, and λ is the wavelength of the optical source. The second splice enlarges the two modes of the PCF and the lead-out SMF recombines them. Note that the splitters in this interferometer are two splices (two zones with collapsed air holes) whose working mechanism is based on diffraction, whereas the arms are two modes, the fundamental LP_{01} mode and a LP_{11}-like higher order mode, that travel at different speeds. Since the splices are high strength and permanent then the long-term reliability of the interferometer is ensured.

The transmission as a function of the wavelength of our interferometer is given by

$$T(\lambda) = I_1(\lambda) + I_2(\lambda) + 2[I_1(\lambda)I_2(\lambda)]^{1/2}\cos(2\pi\Delta nL/\lambda). \tag{1}$$

$I_1(\lambda)$ and $I_2(\lambda)$ are the power of the two modes. The transmission will exhibit a series of maxima and minima with period given by $P\approx\lambda^2/(\Delta nL)$ (see Fig. 2). The maxima appear when $2\pi\Delta nL/\lambda=2m\pi$, being $m=1,2,3\ldots$. This means at wavelengths given by

$$\lambda_m = \Delta nL/m. \tag{2}$$

The thermal behavior of the interferometer is important to analyze before exploring its response to strain. By differentiating Eq. (2) with respect to temperature one gets the shift of the nth interference peak; $\Delta\lambda_n=(\alpha+p_t)\lambda_m\Delta T$, where $\alpha=(1/L)\partial L/\partial T$ is the well-known thermal change of length whose value is $\sim 5\times 10^{-7}/^\circ$C for pure silica, $p_t=(1/\Delta n)\partial(\Delta n)/\partial T$ is the contribution to the thermal change of the difference between the mode indices, and ΔT is the temperature change. Since we have two core modes in the same dopant-free waveguide; therefore a ΔT must affect the two modes in a similar manner for which low temperature dependence was expected. Several interferometers were tested in a temperature chamber (from 22 to 370 °C) and on a hotplate (from 22 to 250 °C). In the samples studied at 1550 nm the temperature sensitivity was found to be in the 3–5 pm/°C range (at $\lambda\sim 850$ nm such values would be even smaller). Such a sensitivity is lower than that of Bragg or long-period gratings or other PCF-based interferometers[4–10] and an order of magnitude lower than the thermal sensitivity of two-mode interferometers based on doped fibers.[15,16]

When the interferometer is subjected to axial strain its length increases by $\delta L(\ll L)$ and the interference pattern shifts to the blue. As a consequence the position of the mth peak changes by $\Delta\lambda_m$. By differentiating Eq. (2) with respect to L we get[17]

$$\Delta\lambda_m = (1+p_s)\lambda_m\varepsilon, \tag{3}$$

where $p_s=(L/\Delta n)\partial(\Delta n)/\partial L$ and $\varepsilon=\delta L/L$. Clearly the shift is a linear function of the applied strain and is additive. It can be noted from Eq. (3) that the shift of the peaks will be larger at longer wavelengths and that it depends weakly on the length of PCF $[p_s\approx(1/\Delta n)\partial(\Delta n)/\partial\varepsilon]$. By assuming that the position of all the maxima are simultaneously monitored, the shift of the interference pattern is then $(\Delta\lambda_m+\Delta\lambda_{m+1}+\Delta\lambda_{m+2}+\cdots+\Delta\lambda_{m+M})/M$, M being the total number of maxima.

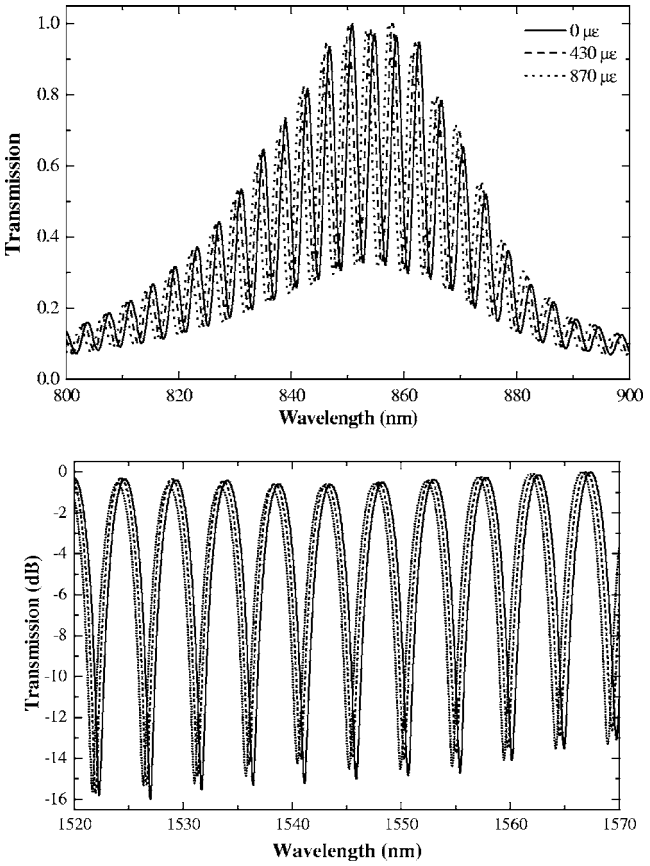

FIG. 2. (a) Normalized transmission spectrum of an interferometer with $L=5$ cm at different strain values. The light source was a low-power LED centered at 850 nm. (b) Normalized transmission spectrum of another interferometer with $L=5.3$ cm at 0 (solid line), $1100\mu\varepsilon$ (dashed line), and $2220\mu\varepsilon$ (dotted line). The light source was an amplified spontaneous emission source.

The analysis above takes into account only two modes and it is supported with the results of Fig. 2(a) and 2(b) where truly sinusoidal patterns at widely separated wavelength ranges of two unstrained and strained interferometers are shown. It is worth noting that the two-mode condition is satisfied at around 850 nm even when the SMF-in/out fiber was a SMF-28 (Corning) which has a cutoff wavelength above 1200 nm. Thus, the interferometer reported here can achieve performances similar to those of an all-PCF interferometer reported recently.[12] In the present case, however, the device is fully compatible with standard fibers and the splices are much stronger, which is critical for long-term reliability. The period of our interferometer is nearly an order of magnitude shorter (therefore much more compact) than those based on high-birefringent PCF.[10,13] In addition, the interference pattern is really stable and immune to drifts or fluctuations of the optical source employed which is important for reliable strain sensing.

Interferometers with different lengths were elongated and compressed several times to verify their reversibility as strain sensors. In Fig. 3 we summarize our results. It is worth

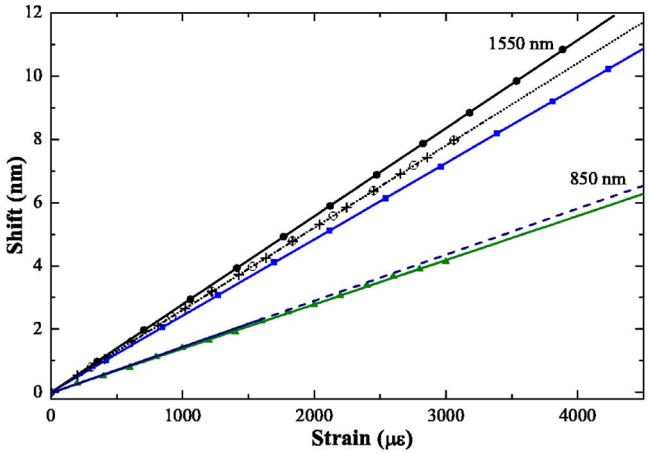

FIG. 3. (Color online) Strain vs shift of the interference pattern at 1550 nm for devices with $L=11.9$ cm (dots) and $L=5.3$ cm (squares) at room temperature. The crosses and circles are shifts at 22 and 94 °C, respectively, for a 10.3 cm long interferometer at 1550 nm. Strain vs shift at 850 nm for devices with $L=12.2$ cm (dashed line) and $L=5.6$ cm (triangles). All the lines are linear fitting to the experimental data.

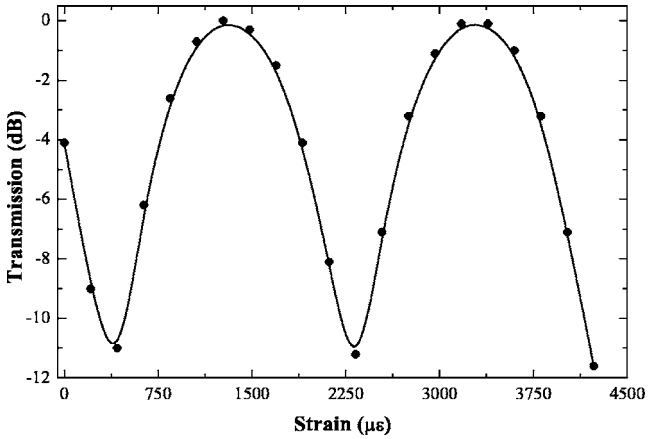

FIG. 4. Normalized transmission of an interferometer with $L=5.4$ cm vs strain. The wavelength was 1549.50 nm. The dots are experimental values and the continuous line is a fitting one. The measurements were carried out at room temperature.

noting that a 10.3 cm long sample exhibits identical behavior at room temperature and at 94 °C. Note also from the figure the linear behavior ($R^2=1$ at 1550 nm and $R^2=0.9996$ at 850 nm) of the sensors. It can be observed from the figure that the shift of the pattern at 1550 nm is above the double than that at 850 nm. L does not have a strong influence on the device sensitivity; the improvement in sensitivity of long devices compared to short ones is less than 15%, which agrees well with the above theoretical analysis. The sensor sensitivities at 1550 and 850 nm are, respectively, 2.80 pm/$\mu\varepsilon$ (when $L=11.9$ cm) and 1.45 pm/$\mu\varepsilon$ (when $L=12.2$ cm). These sensitivities are considerably higher than the typical sensitivity of Bragg grating-based strain sensors ($\sim$1.1 pm/$\mu\varepsilon$). Owing to the high strain sensitivity and the low thermal sensitivity the temperature-induced strain error is calculated to be $\sim$1.5 $\mu\varepsilon$/°C, thus fluctuations of around 20 °C would be needed to induce an error of $\sim$30 $\mu\varepsilon$. Considering the large measurement range of the devices such an error is really low, comparable to the sensor resolution. Therefore temperature compensation would not be necessary if the interferometer is operated in a normal environment. It is worth mentioning that the speed of commercial spectrometers for wavelengths around 850 nm is typically 1 scan/ms for which fast strain sensing can be carried out at such wavelength range.

The interferometer can also be interrogated by launching a fixed wavelength (any in the 800–1600 nm range) and monitoring the output power as a function of the applied strain. In Fig. 4 we show the normalized transmission of an interferometer with $L=5.3$ cm when the wavelength from a tunable laser was fixed at 1549.5 nm. These results show that intensity-modulated strain sensors are also feasible. All these properties combined with the fact that the fabrication of the interferometers is fast and simple make our devices attractive for the development of strain sensors which can be used in a variety of applications.

In conclusion we have reported on interferometric sensing of strain with a photonic crystal fiber fusion spliced to two standard optical fibers. By collapsing the voids of the PCF during the splicing we transform a short section of it into a solid all-silica fiber. Such a solid region broadens the propagating field of the lead-in fiber and allows the coupling of only two modes in the PCF. As strain sensor the device reported here has interesting features such as perfectly linear response, wavelength-encoded information, interferometric working mechanism, broad operating range of wavelengths, low temperature sensitivity, and simple fabrication process. Considering that several physical parameters such as electric fields, vibration, pressure, load, etc., can be translated to strain changes the device proposed here can find use in diverse applications.

This work was carried out with the financial support of the Spanish Ministry of Education and Science through Grant No. TEC2006-10665/MIC/MIC and the "Ramón y Cajal" program, the European Commission through the European Network of Excellence PHOREMOST (FP6-511616), and the Consejo Nacional de Ciencia y Tecnología (Mexico) under Project No. 42986-F.

[1] A. D. Kersey, M. A. Davis, H. J. Patrick, M. LeBlanc, K. P. Koo, C. G. Askins, M. A. Putnam, and E. J. Friebele, J. Lightwave Technol. **15**, 1442 (1997).
[2] H. Ohno, H. Naruse, M. Kihara, and A. Shimada, Opt. Fiber Technol. **7**, 45 (2001).
[3] P. St. J. Russell, J. Lightwave Technol. **24**, 4729 (2006).
[4] L. Zou, X. Bao, S. Afshar V., and L. Chen, Opt. Lett. **29**, 1485 (2004).
[5] C. Martelli, J. Canning, N. Groothoff, and K. Lyytikainen, Opt. Lett. **30**, 1785 (2005).
[6] O. Frazao, J. P. Carvalho, L. A. Ferreira, F. M. Araujo, and J. L. Santos, Meas. Sci. Technol. **16**, 1 (2005).
[7] H. Dobb, K. Kalli, and D. J. Webb, Electron. Lett. **40**, 657 (2004).
[8] Y. P. Wang, L. Xiao, D. N. Wang, and W. Jin, Opt. Lett. **31**, 3414 (2006).
[9] W. J. Bock, W. Urbanczyk, and J. Wójcik, Meas. Sci. Technol. **15**, 1496 (2004).
[10] J. Ju, W. Jin, and M. S. Demokan, IEEE Photonics Technol. Lett. **16**, 2472 (2004).
[11] J. Villatoro, V. P. Minkovich, and D. Monzón-Hernández, Opt. Lett. **31**, 305 (2006).
[12] J. Villatoro, V. P. Minkovich, V. Pruneri, and G. Badenes, Opt. Express **15**, 1491 (2007).
[13] X. Dong, H. Y. Tam, and P. Shum, Appl. Phys. Lett. **90**, 151113 (2007).
[14] H. Y. Choi, M. J. Kim, and B. H. Lee, Opt. Express **15**, 5711 (2007).
[15] A. Kumar, R. Jindal, R. K. Varshney, and S. K. Sharma, Opt. Fiber Technol. **6**, 83 (2000).
[16] Q. Li, C. H. Lin, P. Y. Tseng, and H. P. Lee, Opt. Commun. **250**, 280 (2005).
[17] Y. Liu and L. Wei, Appl. Opt. **46**, 2516 (2007).